A DEFORMATION FAILURE THEORY FOR STACK-BOND BRICK MASONRY PRISMS IN COMPRESSION

R. H. ATKINSON Principal
Atkinson-Noland & Associates, Inc., Boulder, Colorado, USA

J. L. NOLAND Principal
Atkinson-Noland & Associates, Inc., Boulder, Colorado, USA

D. P. ABRAMS, Assistant Professor of Civil Engineering
University of Colorado, Boulder, Colorado, USA

ABSTRACT Compressive tests of stack-bond masonry prisms are used in the United States to evaluate the quality of masonry as a basis for design allowable stresses and as a research experiment. Hence, an understanding of unit-mortar interaction upon prism strength and deformation is important. The multi-axial constituent properties of brick and mortar were determined under carefully controlled conditions for four types of mortar and two types of brick. Using this data a deformation failure theory was developed for stack-bond, solid unit prisms under compressive loading which is based upon nonlinear, dilatent behavior of mortar and linear, elastic behavior of the units. The experimental and analytical work is presented as well as a comparison of calculated vs. predicted prism behavior.

1. INTRODUCTION

Predictions of compressive strength and axial deformation of full scale clay masonry structures are based on compressive tests of stack-bond masonry prisms. The interpretation of the results of prism tests have a significant influence on the allowable stresses and stiffnesses used in masonry design. At present, the mechanisms involved in the deformation and failure of masonry prisms are not fully understood.

Masonry is often assumed to be a homogeneous material in structural design analyses and building code specifications. It's true nature however is determined by a very complex interaction of the mortar, the brick unit, grout and reinforcing steel (if present) and the direction and magnitude of the applied stress state relative to the masonry geometry. Previous investigators (1,2,3) have examined the behavior of the simplest case, that of a stack bond prism of solid unit bricks. Hilsdorf (1) first recognized that masonry failure was governed by an interaction between the mortar and unit although he incorrectly assumed that the mortar was at its failure state when masonry failure occurred. Khoo and Hendry (2) used a maximum lateral strain criterion for the unit as the limiting failure state. Their theory relates unit lateral strain to triaxial stress conditions in the mortar bed joints and assumes strain compatibility between units and mortar.

In the study reported herein a careful examination was made of

the deformation and failure behavior of solid unit, stack-bond prisms. First, the deformational properties and failure conditions of three brick unit types and four mortar types were determined for the expected range and type of multiaxial stress states that these materials would encounter in a prism. Using the measured behavior of the unit and mortar materials as a guide a theory to predict the deformational failure behavior of a stack bond prism under a monotonically increasing vertical compressive load was developed. This theory included force equilibrium and strain compatibility requirements and accounted for observed non-linear and multiaxial material behavior. Using measured material properties in this theory, predictions were made of prism deformation and failure which were compared to results from prism tests. Complete results of this study are contained in Reference 4.

2. BRICK UNIT PROPERTIES

Biaxial tension-compression tests were conducted on clay-units (bricks) to simulate the state of stress of units in a prism under compression. The results of the biaxial tests were used to define the failure envelope used in the theory presented in Section 4.0 predict prism failure. Relatively simple tests such as flatwise compression and indirect tension were also done to determine the basic properties of the three brick types used. The results of these tests were compared to the results of the more complex biaxial tension-compression tests to evaluate the correlation.

2.1 Brick Properties

Three brick types were used in this investigation. These bricks represented a wide range of strengths and physical characteristics. The dimensions of the bricks are shown in Table 1. Types 1 and 3 were bricks typically used in current construction, while Brick Type 2 represented bricks used in many older masonry structures.

The basic properties of each brick type were determined using a standard flatwise one-half unit compressive strength test with and without an interface friction reduction system (IFR) and the initial rate of absorption (IRA) test. The results of these tests are listed in Table 1.

Compressive tests were also done on 22.2 mm diameter brick cores taken normal to the vertical face of the brick. Strain gauges were attached at midheight of the specimen to measure Young's modulus, E, and Poisson's ratio, . Stress-strain plots for each brick type showed that E was constant up to failure while increased slightly with increased vertical stress. The results of these tests are listed in Table 1.

Table 1 Brick Properties

Property	Brick Type 1	2	3
Dimensions (cm)	5.7x9.8x20.0	6.0x10.1x20.3	5.5x8.9x19.4
IRA[1]	19	141	12
Flatwise Comp. Strength (MPa)[2]	102.0	17.1	70.0
Flatwise Comp. Strength (MPa)[3]	58.9	9.4	44.0
22 mm Core Strength (MPa)	67.4	16.6	55.3
Young's Modulus (GPa)	15.0	3.1	9.9
Poisson's Ratio	0.13	0.22	0.17
Indirect Tensile Strength (MPa)	5.57	0.86	2.50
Direct Tensile Strength (MPa)	2.74	0.79	1.79

Notes 1) Initial Rate of Absorption,(ASTM C67-81)[1] , grams/193.55 cm2/min.
2) Std. One-half Unit Compression Test, (ASTM C67-81)
3) One-half unit compression test using the interface friction reduction system

The compressive strength of the 22 mm cores was less than that of the one-half brick specimen and greater than that of the one-half brick specimen tested with interface friction reduction (IFR). The standard-flatwise compressive strength was probably artificially high because of the platen restraint at the compression interface that caused a shear type failure. The cores were sufficiently slender to negate platen effects but could have been affected by the small size of the specimen. The one-half brick specimens in IFR-flatwise compressive tests exhibited a vertical splitting failure similar to the failure of a brick in a prism, but it was not clear whether the IFR induced or allowed the splitting failure. The test method most representative of brick strength could not be determined from these tests.

The tensile strength of the brick was determined with the indirect Brazilian split, and direct tension methods. The Brazilian

[1]American Society for Testing and Materials

split tests were done on 2.5 cm thick disks cut from a 5.4 cm diameter core taken lengthwise through the brick. Specimens were taken from several different bricks, and from various positions within the brick. The specimens were tested so that the tensile split occurred in the vertical plane of the brick from whence the sample was taken.

Entire bricks were used for the direct tensile tests. The tensile load was applied through aluminum brushes to reduce lateral interface shear stresses. The brushes were bonded to the brick using a high strength epoxy and were linked to the tensile frame (Fig. 1), with U-joints to eliminate eccentric load application. The tensile load was applied to the specimen with a hydraulic jack and measured with a Wheatstone strain-gauged bridge mounted on one of the U-joints.

Results of the direct tensile tests and the indirect splitting tests are listed in Table 1. The direct tensile strength method seemed to be a better measure of the tensile strength because it represented the average strength of an entire brick, and generally had less data scatter than the indirect tensile strength method.

A series of biaxial tension-compression tests were done for each brick type. The tensile load was applied in the horizontal plane with the tension apparatus shown in Figure 1. The compressive load was applied to the specimen in the vertical plane through the IFR system with a conventional testing machine.

A minimum of four biaxial tests were done at tensile stress levels of 0.0, 0.25, 0.50, and 0.75 times the average direct tensile strength for each brick type. The tensile load was applied first, followed by an increasing compressive load to brick failure. The tensile load decreased slightly as the compressive load was applied due to the lateral expansion of the brick under compressive loading. The tensile load was monitored and the decrease was included in the results.

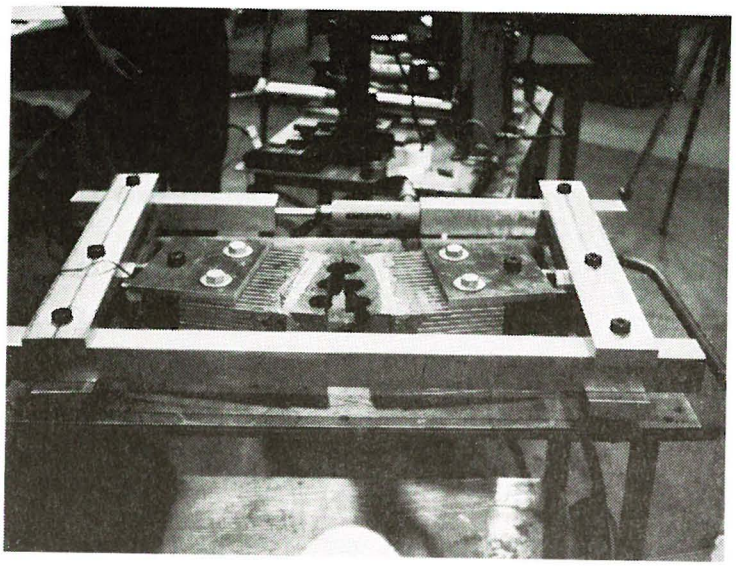

Fig. 1 Tensile Loading Frame

Brick failure generally occurred about 1/2 inch away from the tensile interface in the solid units and through the cores in the cored units. The failures were generally uniform and perpendicular to the direction of the tensile load.

The results of the biaxial tests are listed in Table 2. The IFR flatwise compressive strength (Table 1) was used to define the point of zero tensile load in the biaxial tests. The reason for this was that a IFR was also used in the combined compression-tension tests. A function of the form:

$$\left(\frac{C}{C_o}\right) = 1 - \left(\frac{T}{T_o}\right)^n \qquad \text{for} \quad .5 \leq n \leq 1.0$$

where T is the tensile stress
C is the compressive stress
T_o is the direct tensile strength
C_o is the compressive strength

was used to plot the test data. The data, along with Khoo's (5) test data for the biaxial strength of 1/3 scale model bricks, is plotted in Figure 2.

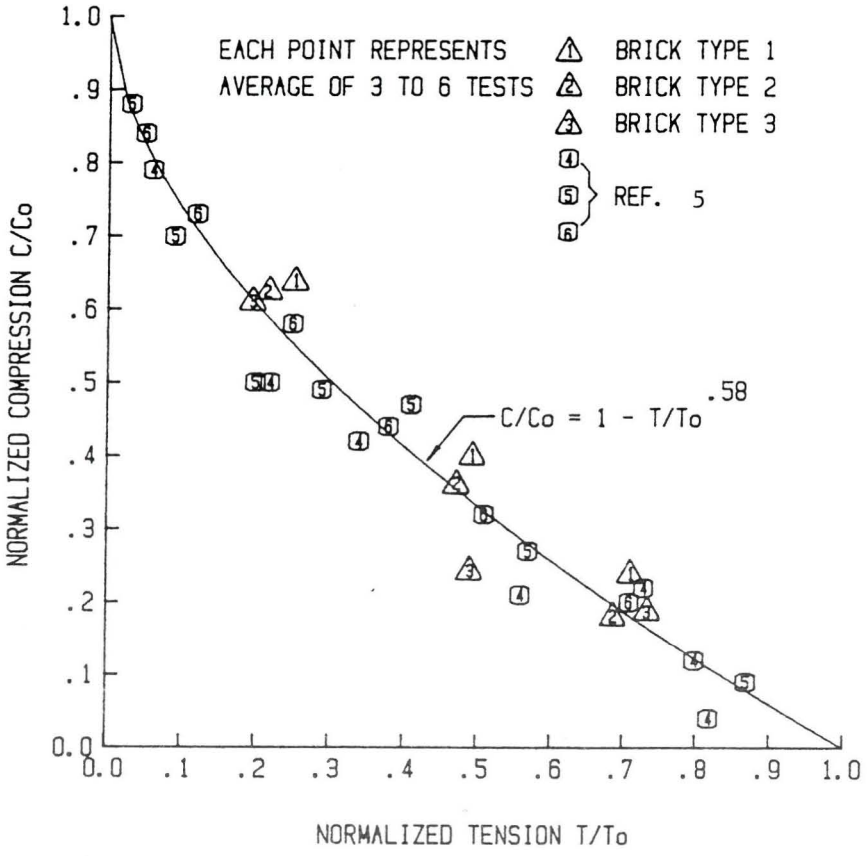

Fig. 2 Nondimensionalized Plot of Biaxial Tension-Compression Brick Tests

Table 2 Results of Biaxial Tension-Compression Brick Tests

Tensile Stress Level	Strength Value	Brick Type[3] 1	2	3
1.0[1]	Ave. Comp. Stress (MPa)	0	0	0
	Ave. Tens. Stress (MPa)	2.74 (10)	0.79 (5)	1.79 (4)
.75	Ave. Comp. Stress (MPa)	14.07 (4)	1.71 (4)	8.22 (6)
	Ave. Tens. Stress (MPa)	1.95	.54	1.32
.50	Ave. Comp. Stress (MPa)	23.64 (6)	3.43 (4)	10.69 (4)
	Ave. Tens. Stress (MPa)	1.35	0.37	0.88
.25	Ave. Comp. Stress (MPa)	37.68 (4)	5.90 (4)	26.85 (3)
	Ave. Tens. Stress (MPa)	0.70	0.17	0.35
0[2]	Ave. Comp. Stress (MPa)	58.86 (5)	9.44 (6)	43.99 (4)
	Ave. Tens. Stress (MPa)	0	0	0

Notes: (1) Direct tensile strength (See Table 1)
(2) Flatwise compressive strength with IFR (See Table 1)
(3) Number in ( ) is number of tests used to calculate average

For this figure, the data are nondimensionalized with respect to the uniaxial compressive strength, C_o, and the average direct tensile strength, T_o, to facilitate comparison of the data of different strength bricks. The data falls in a narrow concave band regardless of brick type and test method. Excellent agreement with Khoo's results is evident.

The coefficient n=0.58 which was obtained by statistical curve fitting indicates that the tensile load had a stronger influence on the compressive strength than the widely used straight line relation assumed by many investigators.

3. MORTAR PROPERTIES

Triaxial compression tests were conducted on four mortar types to determine the deformation and failure properties under stress conditions that would simulate those expected in a mortar joint. The data from these tests was then used as input in the failure model discussed in Section 4.

The four mortars used in this study correspond to commonly used mixes in masonry construction, Table 3. The cement-water ratios listed in Table 3 corresponded to a flow of 110 percent which was determined with a flow table and mold conforming to ASTM C230-68 "Flow Table for Use in Tests of Hydraulic Cement Mortars." The cement-water ratio corresponding to a flow of 110 percent was used to simulate the cement-water ratio of the mortar in a bed joint after loss of water to the brick by suction.

Table 3. Mortar Mixes Used in Study

ASTM Designation	Mortar* Mix	Cement/Water (by weight)
M	1:1/4:3	1.83
S	1:1/2:4-1/2	1.18
N	1:1:6	0.84
O	1:2:9	0.51

*Denotes parts by volume of Portland cement: hydrated lime: masonry sand

The specimens required for the triaxial tests were cylinders 5.4 cm in diameter and 10.8 cm in length. Specimens of 1:1/4:3, 1:1/2:4-1/2 and 1:1:6 mortars were drilled from solid blocks of mortar measuring 10x33x13 cm. Two sets of ten cylinders each were prepared for triaxial tests. The 1:2:9 mortar was too soft to drill from a block, therefore, specimens of this type mortar were cast in individual wooden molds. A total of ten such specimens were prepared for triaxial tests.

The specimens were stripped from the molds after 24 hours in a fog room. They were allowed to cure for 13 more days in the fog room, and then left to air dry until they were tested at 28 days. During the air dry period, the cylindrical specimens were drilled from the blocks, and the tops and bottoms milled flat and parallel. Standard 2-inch cubes were cast in brass molds in accordance with ASTM C109-73.

A modified Hoek-type triaxial cell was used to determine the mortar properties. The lateral expansion of the specimen at midheight, as well as the axial deformation was measured. Lateral confining pressure was exerted on the specimen by hydraulic fluid acting through a plastic membrane, while a ram inserted through the top of the cell exerted the axial load. A servo-controlled testing machine was used to load the specimen at a constant displacement rate.

This triaxial cell was well suited for these mortar tests for the following reasons: (1) the axial and lateral expansions were measured by mechanical means up to and past the ultimate vertical load, (2) the specimen was surrounded by a membrane, and did not require a surface sealant, and (3) a constant confining pressure could be applied to the specimen.

The mortar specimens were tested at confining pressures of 0.2, 0.7, 1.7, 3.5, 6.9, and 10.3 MPa. Generally, one or two tests at each confining pressure were conducted on the first set of 10 specimens. The second batch of 10 specimens for a particular mortar type was tested at various cell pressures to substantiate any questionable results from tests using the first mortar specimens. Usually, 3 or 4 tests were run at each level of lateral pressure for each mortar type.

The load path followed in the triaxial tests was to first apply the lateral pressure (σ_3) and then load the specimen axially at a deformation rate approximately equal to .0001 strain/sec. The lateral pressure was maintained constant as the specimen was loaded axially past its peak strength into residual or post-peak behavior. Continuous plots of axial load and lateral deformation vs. axial deformation were obtained.

Triaxial Test Results

Representative stress-strain curves for each confining pressure are plotted on a common axis for the 1:1/2:4-1/2 and 1:1:6 mortars in Figure 3. For all tests, the ultimate load and ultimate strain increased with increased confining pressure, while the ultimate lateral strain decreased with increased confining pressure. The stress-strain plots for the 1:1/2:4-1/2 mortar clearly show the transition from brittle behavior at low confining pressure levels to ductile behavior at high confining pressure levels. For the weaker mortars a bi-linear behavior was observed for the higher levels of confining pressures as illustrated in Figure 3b. A characteristic of all mortars at all confining pressures is the non-linear stress-strain behavior at loads that exceed approximately 50% of ultimate load.

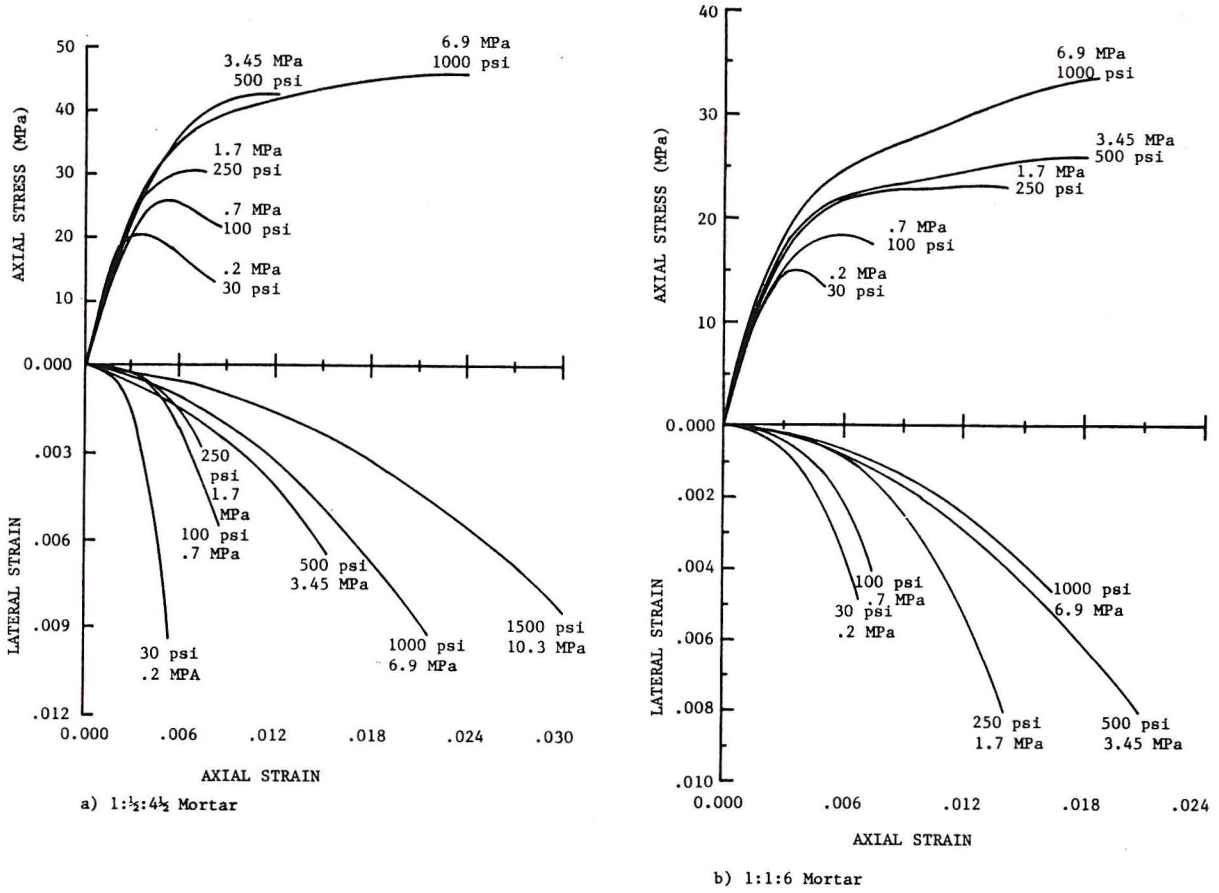

Fig. 3 Representative Mortar Stress-Strain Plots

The ultimate load was plotted versus confining pressure in Figure 4. As shown in this figure, the ultimate-strength envelope can be represented with a straight line for each mortar type.

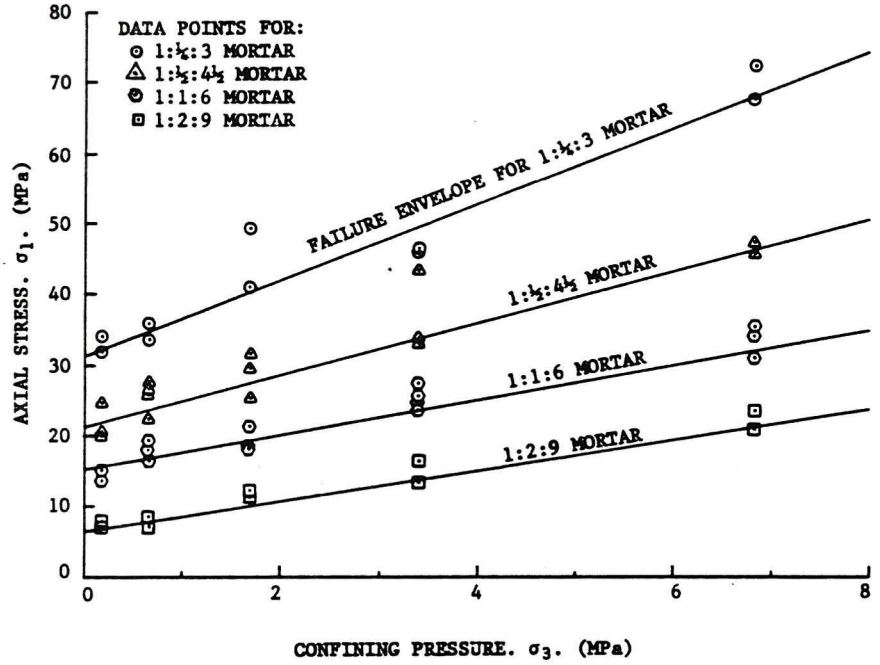

Fig. 4 Ultimate Strength Envelopes for the Four Mortar Types Tested

Values of the elastic modulus, E, and Poisson's ratio were plotted versus axial stress for each confining pressure as illustrated in Figure 5 for the 1:1/2:4-1/2 mortar. It was observed that for confining pressures less than 100 psi, the value of E decreased quite slowly, then dropped quickly with increased axial stress. The values of E tended to drop constantly as axial stress increased for higher values of confining pressure. This trend was most pronounced in the weaker mortar mixes. It was observed that Poisson's ratio was large for the strong mortars at low confining pressures. Conversely, Poisson's ratio was relatively low for the weaker mortars at high confining pressures.

The series of mortar tests described led to a better understanding of mortar under triaxial compression. Several observations can be made:

(1) All four mortar types tested exhibited nonlinear behavior.
(2) The ultimate strength and ultimate axial strain increased with increased confining pressure.
(3) The ultimate strength envelope can be represented with a linear Coulomb relation.
(4) The confining pressure has a strong influence on the magnitude and variation of the elastic modulus and

(5) The mechanical properties of the 1:2:9 and the 1:1:6 mortar change significantly under high confining pressures.

(6) Compressive strength, Poisson's ratio, and Young's modulus of the mortar were strongly influenced by relative cement content.

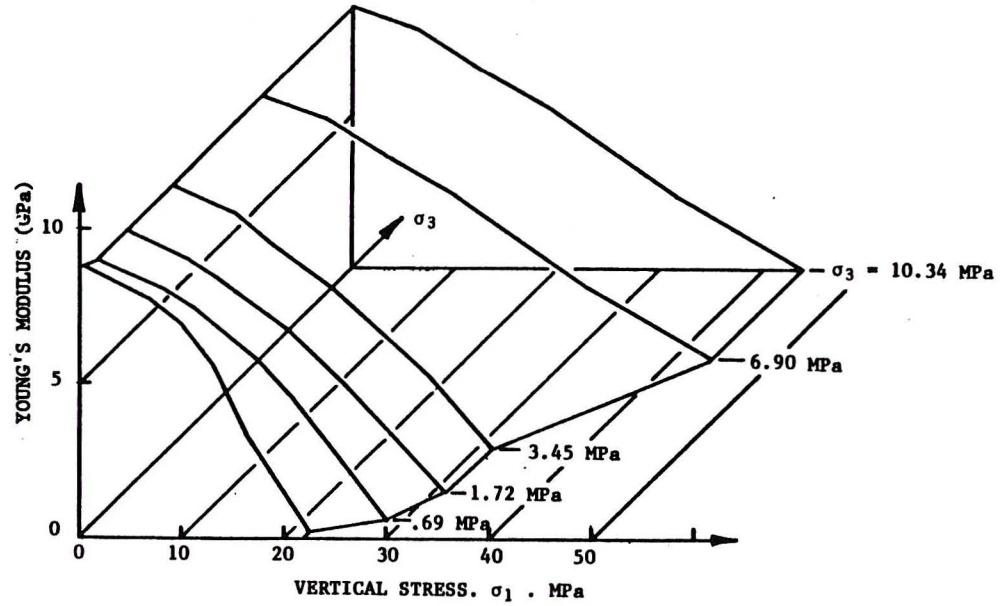

a) Young's Modulus vs σ_1 & σ_3

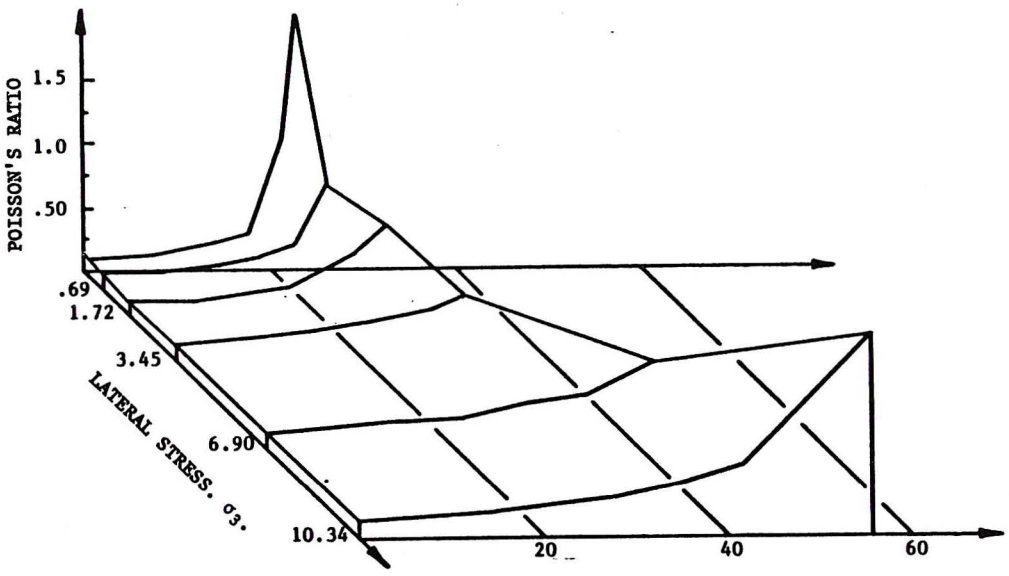

b) Poisson's Ratio vs σ_1 & σ_3

Fig. 5 Elastic Parameters vs σ_1 and σ_3 for 1:1/2:4-1/2 Mortar

4. DEVELOPMENT OF THEORY

A theory for the deformation and failure of a stack bond masonry prism under a compressive load was developed, Atkinson and Noland (6). The theory builds on the work of Hilsdorf (1) and Khoo and Hendry (2) by including the non-linear dilatent behavior of the mortar in an interactive solution scheme and is described as follows:

Consider a column of alternating layers of brick and mortar (Figure 6). Assume that both the brick and mortar are subject to a uniform vertical compressive stress, σ_1, and that the lateral stresses in both the brick and mortar are uniform. Equilibrium of force in the lateral direction requires that:

$$\sigma_{xm} t_m + \sigma_{xb} t_b = 0 \ , \tag{1}$$

provided adequate shear bond exists between the mortar and brick.

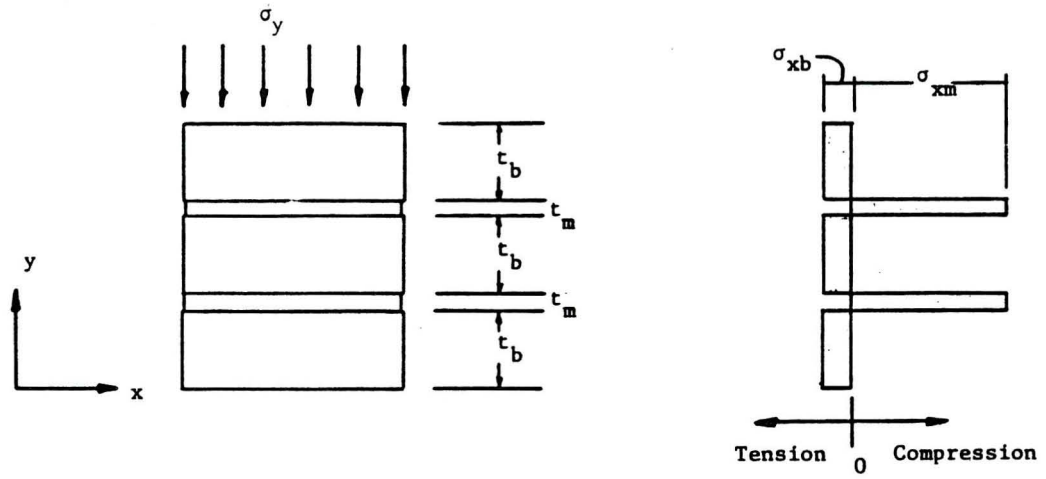

Fig. 6 Stack Bond Prism Stress Distribution

Assume, using a compatibility argument, that equal lateral strains exist in the brick and the mortar:

$$\varepsilon_{xb} = \varepsilon_{xm} \ . \tag{2}$$

The non-linear behavior of the mortar, as illustrated in Figures 3 and 5 can be expressed as functions of the major principal stress, σ_1, and the confining stress, σ_3, i.e.,

$$\begin{aligned} E_m &= f(\sigma_1\ \sigma_3) \\ \nu_m &= f(\sigma_1\ \sigma_3) \end{aligned} \tag{3}$$

where, for the masonry prism (Figure 6), the principal stress, σ_1, corresponds to the vertical compressive stress, σ_y, and the principal stress, σ_3, corresponds to the lateral mortar compressive stress, σ_{xm}. The elastic parameters for the brick, E_b and ν_b, are constant values.

From isotropic elasticity theory the lateral strain increment resulting from an applied vertical load increment, $\Delta\sigma_y$, will be,

$$\Delta\varepsilon_{xb} = \frac{1}{E_b}\left[\Delta\sigma_{xb} - \nu_b\Delta\sigma_y\right] \tag{4}$$

$$\Delta\varepsilon_{xm} = \frac{1}{E_{m(\sigma_1,\sigma_3)}}\left[\Delta\sigma_{xm} - \nu_{m(\sigma_1,\sigma_3)}\Delta\sigma_y\right] \tag{5}$$

Substituting in the previously developed expressions for equality of lateral strain and lateral force equilibrium, the following expression for lateral brick stress is derived,

$$\Delta\sigma_{xb} = \frac{\Delta\sigma\left[\nu_b - \frac{E_b}{E_{m(\sigma_1,\sigma_3)}}\nu_{m(\sigma_1,\sigma_3)}\right]}{1 + \frac{E_b}{E_{m(\sigma_1,\sigma_3)}}\frac{t_b}{t_m}} \tag{6}$$

A computer routine has been written to evaluate the lateral brick and mortar stress as the vertical load is increased incrementally, summing the lateral stress increments from each load increment. The masonry (prism) is assumed to fail when either mortar failure in triaxial compression or brick failure in axial compression-lateral tension occurs. These failure envelopes are input either in a linear form or in a non-linear form and the program checks, after each load increment, the biaxial stress state of the brick and mortar against their prescribed failure envelope.

5. COMPARISON OF PRISM TEST RESULTS TO THEORETICAL PREDICTIONS

5.1 Prism Tests

Uniaxial compression tests were conducted on five unit stack-bond prisms built from the three brick types and four mortar types previously described. The prisms were built in accordance with ASTM C-67 using a special prism construction jig which eliminated much of the variability inherent in hand made prisms.

The prisms were cured for seven days in a fog room and then air cured for 21 days until tested. The prisms were capped using a gypsum cement material and tested using an interface friction reduction system (IFR). Axial deformation was measured using LVDT's attached to the top and bottom bricks of the five unit prism.

Prisms were loaded at a rate of approximately 0.0001 strain/min. in a conventional testing machine. The failure mode of prisms tested using the IFR system was generally a vertical splitting down the narrow face followed shortly by total collapse.

5.2 Predicted Prism Behavior

The compressive strengths of prisms modeled with each combination of three brick types and four mortar mixes were calculated using the computational model outlined previously. For each

brick-mortar combination, the model predicted that failure occurred in the brick. The ultimate strengths of prisms calculated using the computational model are listed in Table 4.

Table 4. Comparison of Measured and Calculated Prism Strengths

Brick Type	Mortar Type	Prism Strength (MPa) Measured	Calculated
1	1:1/4:3	48.2	34.2 (71%)*
	1:1/2:4-1/2	40.9	28.8 (70%)
	1:1:6	32.5	25.8 (79%)
	1:2:9	29.9	18.1 (60%)
2	1:2:9	6.4	5.6 (88%)
3	1:1/4:3	37.7	23.8 (63%)
	1:1/2:4-1/2	34.7	21.9 (63%)
	1:1:6	27.0	17.7 (65%)
	1:2:9	19.7	13.7 (69%)

*Figures in brackets are percentage of measured strength.

Though the calculated prism strengths were consistently lower than the measured strengths, the computational model did successfully predict the relative changes in compressive strength for prisms built with a given brick type and each of four mortar types. The computational model worked equally well for cored clay units (Brick Type 3) and solid clay units (Brick Type 1). One possible reason for the lower strength predicted by the theory is that the theory only predicts the occurrence of the first vertical crack in the brick unit rather than the ultimate collapse load measured in the prism tests. Audible cracking sounds were often observed at approximately 80% of ultimate load with visible vertical cracks apparent at 90% to 95% of ultimate.

The experimentally measured axial deformations were compared to the calculated axial deformations for each prism type.

The stress-strain curves based on experimentally measured deflections (LVDT's mounted on the prism) were quite similar to those based on the deflections calculated using the computational model. Though the calculated strains were consistently greater than the measured strains, the stress-strain curves based on measured and calculated deflections were similar in shape for all prism types modeled. For example, stress-strain curves based on calculated and measured deflections of a prism consisting of Brick Type 1 and 1:1/4:3 mortar (Figure 7) were both essentially linear up to failure and had similar slopes. The stress-strain curves of a prism modeled with the same brick type and 1:2:9 mortar both showed significant softening due to the nonlinear behavior of the weaker 1:2:9 mortar.

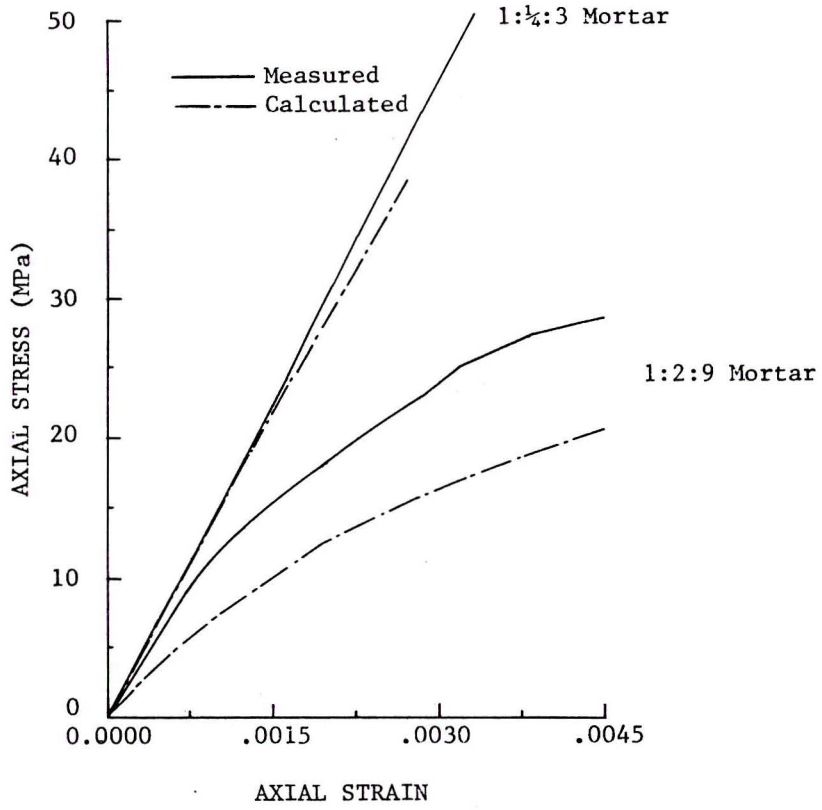

Fig. 7 Predicted vs Measured Prism Stress-Strain Curves, Brick Type 1

The lateral stress in the brick and mortar calculated using the computational model was plotted as a function of vertical stress for prisms modeled with Brick Types 1 ,2, and 3. For a given brick type, the stress curves for the brick and the mortar were increasingly nonlinear as the mortar strength decreased (Figure 8). This meant that the mortar stress curve did not cross the mortar failure envelope even for a prism modeled with the weakest mortar (1:2:9) and the strongest brick (Brick Type 1) (Figure 8b). This indicated that failure was always initiated in the brick and was consistent with the observed mode of failure in test prisms.

6. SUMMARY AND CONCLUSIONS

This research study had as its purpose the development and evaluation of a theory to predict the strength and deformation of stack-bond clay unit masonry under compressive loading. The theory sought to incorporate expressions for the multi-axial deformation and failure of the brick and mortar. The development and verification of the theory as well as the experimental work devoted to measuring material properties provided increased insight into the actual mechanisms associated with masonry behavior. These mechanisms reflect the complex interaction that occurs between the mortar and the brick under compressive load. The non-linear dilatent behavior of the mortar was shown to have a significant influence in determining masonry failure levels.

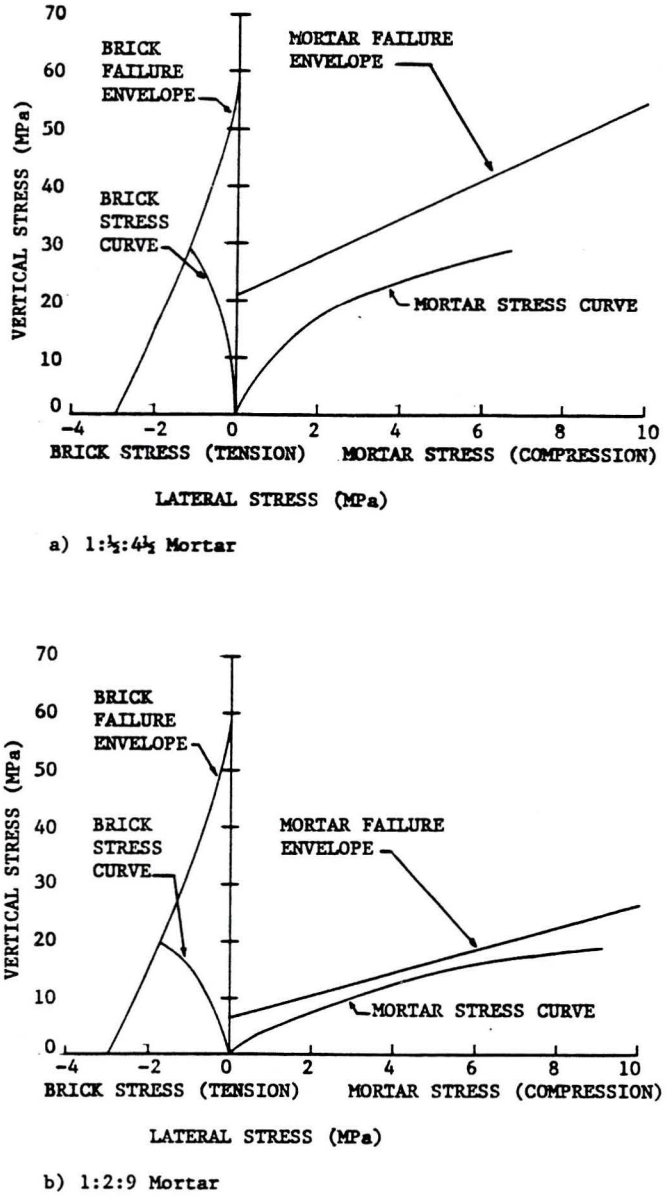

Fig. 8 Calculated Stresses in Brick and Mortar for Prisms Modeled with Brick Type 1

7. ACKNOWLEDGEMENT

The experimental results reported in this paper are based on work of W.S. McNary and form part of his M.S. Thesis at the University of Colorado. This effort was funded by the National Science Foundation as part of a joint Industry/University cooperative effort by Atkinson-Noland & Associates, Inc. (Grant CEE-8115002) and the University of Colorado (Grant CEE-8115005).

8. REFERENCES

(1) HILSDORF, H.K., "Investigation into the Failure Mechanism of Brick Masonry Loaded in Axial Compression," Proceedings of International Conference on Masonry Structural Systems, Gulf Publishing Co., Houston, Texas, 1969, pp. 34-41.

(2) KHOO, C.L. and A.W. HENDRY, "A Failure Criteria for Brickwork in Axial Compression," Proceedings of Third International Brick Conference, Essen, England, 1973, pp. 141-145.

(3) SHRIVE, N.G. and E.L. JESSOP, "Anisotropy in Extruded Clay Units and Its Effect on Masonry Behavior," Proceedings of Second Canadian Masonry Symposium, Ottawa, Canada, 1980, pp. 39-50.

(4) McNARY, W.S., R.H. ATKINSON, J.L. NOLAND and D.P. ABRAMS, "Basic Properties of Clay-Unit Masonry in Compression," Report to National Science Foundation, Atkinson-Noland & Associates, Inc., Report ANA R8213-1, 1984.

(5) KHOO, C.L., "A Failure Criterion for Brickwork in Axial Compression," Ph.D. Thesis, University of Edinburgh, Edinburgh, Scotland, 1972.

(6) ATKINSON, R.H. and J.L. NOLAND, "A Proposed Failure Theory for Brick Masonry in Compression," Proc. 3rd Canadian Masonry Symposium, Edmonton, 1983.